Oncogene (2002) 21, 7545–7556
© 2002 Nature Publishing Group All rights reserved 0950–9232/02 $25.00
www.nature.com/onc

Post-transcriptional regulation of cyclin D1 expression during G2 phase

Yang Guo[1], Dennis W Stacey[1] and Masahiro Hitomi*[,1]

[1]*The Department of Molecular Biology, NC2-150 The Lerner Research Institute, The Cleveland Clinic Foundation, 9500 Euclid Avenue, Cleveland, Ohio, OH 44195, USA*

During continuous proliferation, cyclin D1 protein is induced to high levels in a Ras-dependent manner as cells progress from S phase to G2 phase. To understand the mechanism of the Ras-dependent cyclin D1 induction, cyclin D1 mRNA levels were determined by quantitative image analysis following fluorescent *in situ* hybridization. Although a slight increase in mRNA expression levels was detected during the S/G2 transition, this increase could not explain the more robust induction of cyclin D1 protein levels. This suggested the involvement of post-transcriptional regulation as a mechanism of cyclin D1 protein induction. To directly test this hypothesis, the cyclin D1 transcription rate was determined by run-on assays. The transcription rate of cyclin D1 stayed steady during the synchronous transition from S the G2 phase. We further demonstrated that cyclin D1 protein levels could increase during G2 phase in the absence of new mRNA synthesis. α-Amanitin, a transcription inhibitor, did not suppress cyclin D1 protein elevation as the cells progressed from S to G2 phase, even though the inhibitor was able to completely block cyclin D1 protein induction during reentry into the cell cycle from quiescence. The half life of cyclin D1 protein was shortest during S phase indicating that a change in protein stability might play a role in post-translational induction of cyclin D1 in G2 phase. These data indicate a fundamental difference in the regulation of cyclin D1 production during continuous cell cycle progression and re-initiation of the cell cycle.
Oncogene (2002) **21,** 7545–7556. doi:10.1038/sj.onc.1205907

Keywords: cell cycle; Ras; cyclin D1; *in situ* hybridization; single cell-based analysis; post-transcriptional regulation

Introduction

Cell cycle progression consists of multiple coordinated processes, including DNA duplication and chromosome segregation, to ensure accurate transfer of genetic information to daughter cells. To achieve this, cells are equipped with a variety of systems to sense unfavorable conditions for completing the cell cycle, such as lack of mitogens, low nutrient levels, DNA damage, disruption of the mitotic spindles, etc. Under such conditions, check points are activated and cell cycle progression is halted at specific points in the cell cycle (Pardee, 1989; Vogelstein *et al*., 2000). Some of these reversible checkpoints have been utilized to synchronize cells to study cell cycle regulation. To study the control of G1/S phase transition, for instance, mitogen deprivation-readdition is often employed. When mitogens are removed, mammalian fibroblast cells are arrested in a quiescent state, referred to as G0, with a G1 content of DNA. This withdrawal from the cell cycle may have physiological importance, because forced cell cycle progression in the absence of growth factors often results in apoptosis (Evan and Vousden, 2001). When mitogens are available again, the cells reenter into cell cycle. The reversible nature of this G0 arrest has allowed studies of the molecular events controlling the cell cycle transition from G0 to S phase, as summarized below.

During reentry into the cell cycle, Ras plays an essential role to transmit proliferative signaling from growth factors to cell cycle progression (Mulcahy *et al*., 1985). Upon mitogenic stimulation, Ras binds GTP and activates multiple downstream target molecules, including the mitogen activated protein kinase (MAP kinase) pathway. Activated MAP kinases phosphorylate and activate transcription factors such as AP-1 and the Ets family. These transcription factors stimulate many target genes including cyclin D1, whose promoter contains AP-1 and Ets binding sites. These elements are required for Ras-dependent activation of the cyclin D1 promoter (Albanese *et al*., 1995). Other downstream pathways of Ras signaling, such as phosphatidylinositol 3-kinase (PI3 kinase) and the Ral pathway, also induce cyclin D1 transcription (Gille and Downward, 1999). Induced cyclin D1 protein forms active Rb kinase complexes with cdk4 or cdk6, and promotes cell cycle transition from G1 to S phase (Degregori *et al*., 1995; Sherr, 1995).

The above model was elucidated from observation of synchronous cultures reentering the cell cycle from quiescence. There are lines of evidence, however, that the molecular events regulating the G1/S transition of continuously cycling cells might be different from those involved in the G0/S transition. For instance, c-*myc* expression levels transiently peak during the transition from G0 to S phase, while such a peak is not detected in continuously proliferating cells (Hann *et al*., 1985;

*Correspondence: M Hitomi; E-mail: hitomim@ccf.org
Received 30 January 2002; revised 11 July 2002; accepted 18 July 2002

Thompson *et al*., 1985). c-Fos is only required for quiescent cells to enter S phase but not in continuously cycling cells (Kovary and Bravo, 1992). Cdc6, an E2F target molecule essential for DNA replications, is expressed at very low levels in G1 phase from quiescence, but it is expressed at high levels throughout the cell cycle in proliferating cultures (Yan *et al*., 1998). Therefore, observations of quiescent cultures reentering the cell cycle may not always be applicable to G1/S transition in rapidly cycling cells.

We previously developed a method to analyse cell cycle progression without synchronization by combining time lapse, quantitative fluorescent microscopy and microinjection (Hitomi and Stacey, 1999a,b; Stacey *et al*., 1999, 2000). This approach revealed that in asynchronous NIH3T3 cell cultures, cyclin D1 is induced in a Ras-dependent manner during cell cycle transition from S to G2 phase. Once induced in G2 phase, cyclin D1 expression became Ras independent through the next G1 phase. Expression of cyclin D1 during G1 phase is essential for the G1/S phase transition of continuous cell cycle progression. In this way, when cells are continuously cycling, a Ras-dependent decision for the next cell is made during G2 phase (Hitomi and Stacey, 1999a,b, 2001). In this study, we demonstrate that the Ras-dependent induction of cyclin D1 during cell cycle transition from S to G2 phase is mediated by a post-transcriptional mechanism.

Results

Cyclin D1 mRNA detection with fluorescent in situ *hybridization*

As proliferating cells progress from S to G2 phase, cellular Ras activity induces cyclin D1 protein expression from the low levels of S phase cells to higher levels. Once induced, cyclin D1 is expressed at high levels through the next G1 phase in a Ras-independent manner (Hitomi and Stacey, 1999b). In order to understand the mechanism underlying this Ras-dependent cyclin D1 induction during the S/G2 transition, we first determined the levels of cyclin D1 mRNA. For this purpose, we used quantitative digital image analysis of fluorescent *in situ* hybridization to determine mRNA levels throughout the cell cycle. Such a single-cell based analysis was necessary because the expression patterns of cyclin D1 in asynchronous culture might be different from the patterns observed in synchronous cell cycle progression following release from growth arrest (Hitomi and Stacey, 2001).

First we tested the specificity of the probes. When NIH3T3 cells were examined with sense oriented probe for cyclin D1, little signal was detected. Antisense probe, in contrast, hybridized mainly to the cytoplasmic area to give strong fluorescent signals (Figure 1A, a and b). When the cells from a cyclin D1 knockout mouse (Sicinski *et al*., 1995) were probed, very low signal was detected even with anti-sense probe (Figure 1A, c and d). These data indicate that the anti-sense probe can specifically detect cyclin D1 mRNA. Similar strong signals were detected with anti-sense probes for GAPDH and histone H3 in comparison to the signals obtained with sense oriented probes (data not shown).

Next we examined the relationship between cyclin D1 mRNA content and fluorescent intensity determined by image analysis of fluorescent *in situ* hybridization. For this purpose, cyclin D1 mRNA levels in synchronous NIH3T3 cells were determined by image analysis of fluorescent *in situ* hybridization (Figure 1B,D). The levels of cyclin D1 mRNA associated fluorescence were determined by image analysis and compared to the cyclin D1 mRNA levels determined at the same time by Northern blot analysis (Figure 1C,D). The level of cyclin D1 expression was normalized to GAPDH mRNA level in both methods. As shown in Figure 1D, image analysis of fluorescent *in situ* hybridization yielded results proportional to those of Northern blot analysis. This indicates that mRNA expression levels in individual cells can be quantitatively determined by digital image analysis of fluorescent *in situ* hybridization.

Cyclin D1 message levels oscillate less than protein through the cell cycle

Cyclin D1 mRNA expression throughout the cell cycle was determined by quantitative fluorescent *in situ* hybridization. The cell cycle phase of individual cells was determined by the intensity of DAPI staining and the incorporation of BrdU as described (Hitomi and Stacey, 1999b). We determined the ratio of total mRNA vs total DNA in order to correct for the general increase in expression associated with progression through the cell cycle (Stacey *et al*., 2000). Although the expression levels of cyclin D1 mRNA were distributed in a wide range (Figure 2B), the levels were generally higher in G1 phase, slightly lower in S phase, and higher in G2 phase. In order to compare the expression levels in each cell cycle phase, cells were grouped according to cell cycle phase and fluorescence levels were averaged. S phase was divided into two halves because the expression of cyclin D1 tended to be higher at the beginning of S phase than in late S phase. The average DNA value among S phase cells (BrdU positive cells) was calculated. The S phase cells with DNA less than this were grouped as S1 (early S phase cells), and the rest of the S phase cells were grouped as S2 cells (late S phase cells). As shown in Figure 2C, the expression level of cyclin D1 mRNA was the highest in G1 phase, declined slightly through S phase to reach the lowest levels in late S phase (S2), and then increased slightly again in G2 phase. To confirm that this profile of cyclin D1 mRNA expression was not due to the technical limitation of fluorescent *in situ* hybridization, we applied the method to monitor histone H3 mRNA, whose expression is highest during S phase (Delisle *et al*., 1983; Dirks and Raap, 1995; Rickles *et al*., 1982). As expected, high expression of histone H3 mRNA was detected among BrdU positive S phase cells (Figure 3A). When the levels of histone H3 mRNA was determined and plotted against DNA

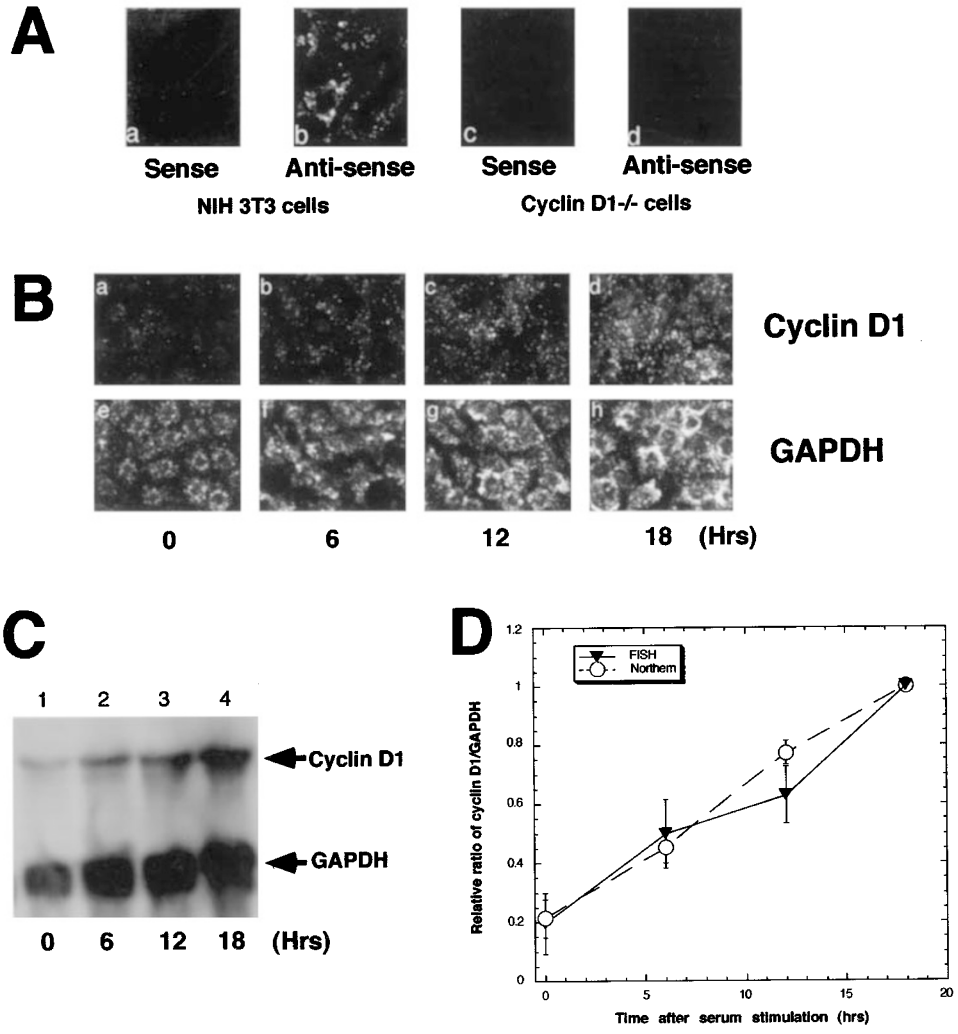

Figure 1 Quantitative fluorescent *in situ* hybridization. (**A**) NIH3T3 cells (a and b) and cyclin D1 knockout mouse embryonic fibroblasts (c and d) were plates on coverslips. After fixation, they were probed with digoxigenin labeled sense (a and c) or anti-sense (b and d) probes for cyclin D1. Hybridized probes were visualized by anti-digoxin antibody with fluorescent signal amplification. (**B**) NIH3T3 cells grown on coverslips were made quiescent by serum starvation for 2 days. They were stimulated with 10% serum to reinitiate the cell cycle. Cells were fixed before (a and e), or 6 h (b and f), 12 h (c and g), and 18 h (d and h) after serum addition. The cyclin D1 (a–d) or GAPDH (e–h) messages were detected by fluorescent *in situ* hybridization. (**C**) NIH3T3 cells were deprived of serum for 2 days to synchronize them at G0. Before (0 h, lane 1) or 6 (lane 2), 12 (lane 3), or 18 h (lane 4) after re-stimulation with serum, total RNA was prepared and 20 μg of RNA for each time point was analysed by Northern blot analysis. Cyclin D1 and GAPDH messages were detected with digoxigenin labeled anti-sense RNA probes simultaneously. The hybridized probes were visualized with a Storm Imager using chemiluminescense. (**D**) Comparison between fluorescent *in situ* hybridization and Northern blot. Fluorescence levels of *in situ* hybridization were determined by image analysis of digital microscopic images. The amount of mRNA detected by the Northern blot was determined by integrating the pixel density of digital images collected by the Storm Imager. At each time point, the average cyclin D1 fluorescence was divided by the average GAPDH fluorescence of 300–500 cells. Each ratio obtained for each time point was normalized against the ratio value at 18 h. The average values of normalized ratios were calculated from three independent experiments and plotted (closed triangles) with standard errors indicated with error bars. For comparison, the data obtained from three separate Northern blot analyses were processed in the same way and plotted (open circle)

content, its expression profile was almost indistinguishable from the BrdU incorporation pattern (Figure 3B,C). This expression pattern is in good agreement with the literature (Delisle *et al*., 1983; Dirks and Raap, 1995; Kotelnikov *et al*., 1997; Rickles *et al*., 1982), indicating the reliability of quantitative fluorescent *in situ* hybridization.

The cyclin D1 protein expression levels (total D1 protein divided by DNA content), on the other hand, showed a much larger change during cell cycle progression than mRNA levels (Figure 2A,C). The protein level was highest in G1 phase cells, and declined dramatically during S phase, with lowest levels later in S phase. There was a 2–2.5-fold increase in protein levels as the cells progressed from late S phase. In contrast, the induction of mRNA was only about 1.3-fold during S/G2 transition (Figure 2C).

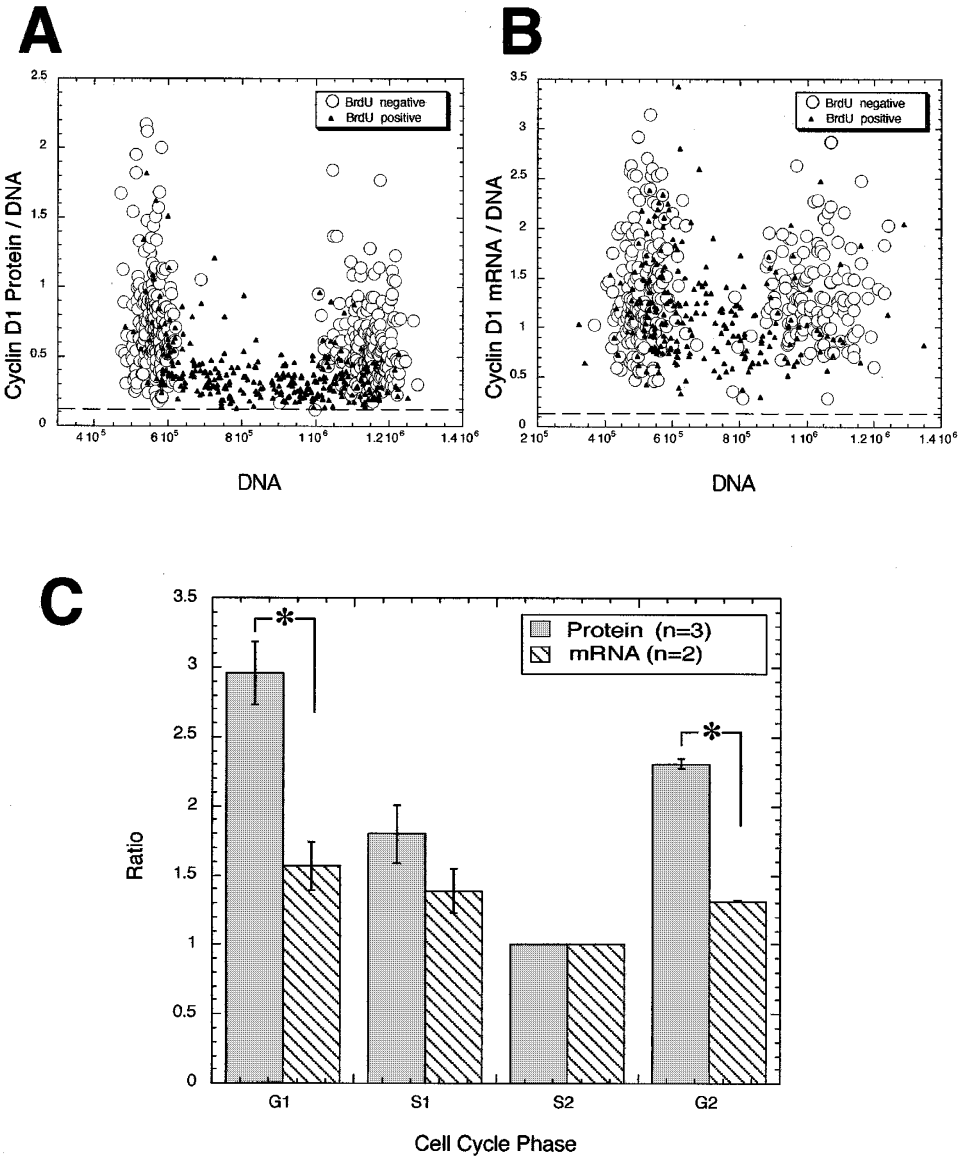

Figure 2 Cyclin D1 protein and mRNA expression through the cell cycle. (**A**) NIH3T3 cells were pulse labeled with BrdU for 30 min prior to staining for cyclin D1 protein by indirect immunofluorescence. (**B**) In a parallel plate, Cyclin D1 message was detected by fluorescent *in situ* hybridization using a specific anti-sense probe for cyclin D1 mRNA. Both monolayers were re-fixed to detect incorporated BrdU by immunostaining. After DNA was stained with DAPI, digital images were captured to determine the fluorescence intensity of cyclin D1 mRNA, D1 protein, BrdU and DNA. To determine the background signal levels for protein staining and message detection, the cells were probed with non-immune mouse IgG or a sense oriented probe. The ratio of cyclin D1 protein/DNA, or cyclin D1 mRNA/DNA for each cell was plotted against DNA content. The dotted lines at the bottom indicate the background staining levels determined in parallel plates stained with non-immune IgG, or probed with sense oriented probe. In both plots, open circles are BrdU negative cells and closed triangles are BrdU positive cells. (**C**) To compare cyclin D1 protein and mRNA levels, cells were grouped according to their DNA content and BrdU labeling state into four groups, G1, S1 (early S phase), S2 (later S phase) and G2 (see Materials and methods). For each group, the average value of fluorescence levels divided by the DNA content were calculated to correct for the generalized increase in expression level associated with cell size increase through the cell cycle. The ratio value for late S phase cells was arbitrarily set to 1.0, and relative values for other cell cycle phases are presented. The mean values for relative ratios of mRNA/DNA and protein/DNA were determined from duplicated *in situ* hybridization and triplicated immunostaining experiments. The error bars represents standard error. Asterisks indicate statistically significant differences detected by *t*-test ($P<0.05$)

Steady transcription rate

The discrepancy between the expression levels of mRNA and protein suggests an involvement of post-transcriptional regulation for this Ras-dependent cyclin D1 protein induction in G2 phase. Ras, however, has been reported to induce cyclin D1 transcription through MAP kinase (Albanese *et al*., 1995) or other downstream pathways (Gille and Downward, 1999). Therefore, we carefully examined the cell cycle dependent change of cyclin D1

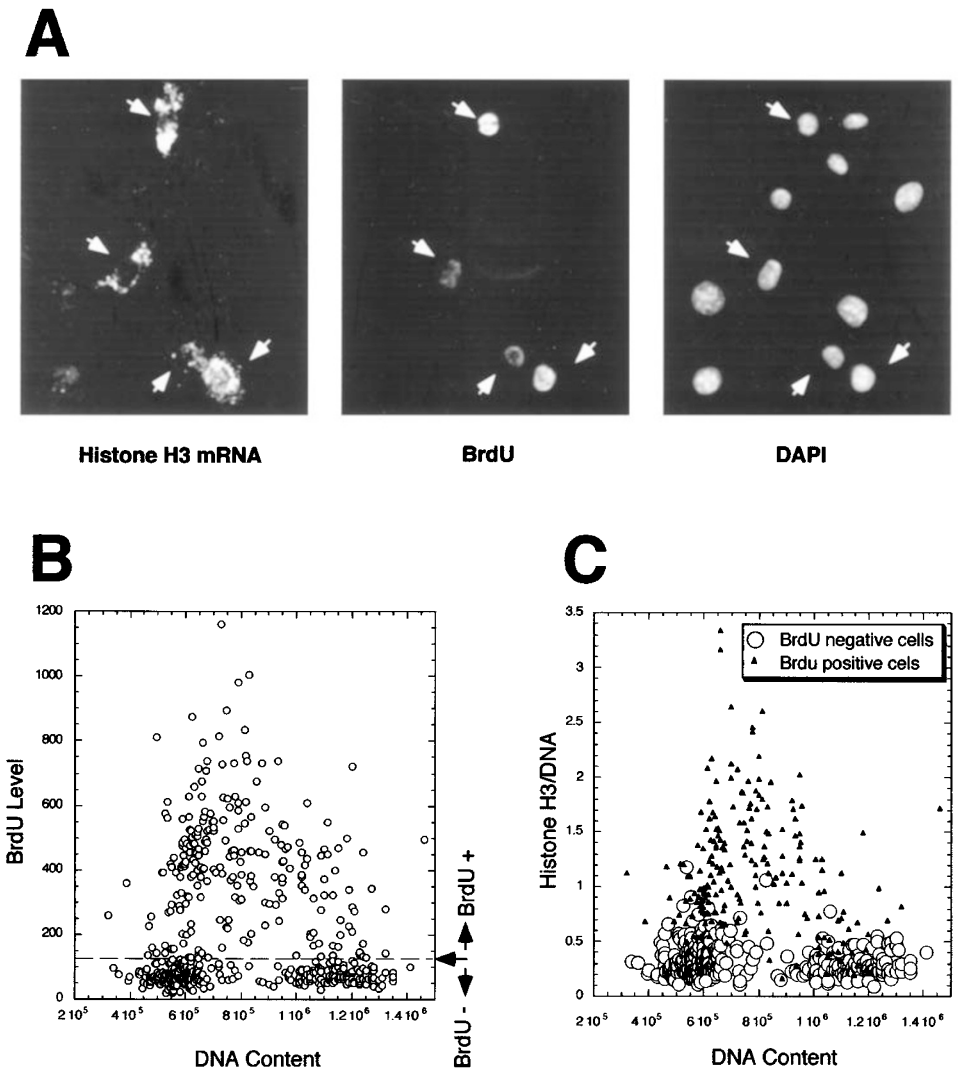

Figure 3 Histone H3 message expression. Rapidly proliferating NIH3T3 cells were pulsed with BrdU for 30 min and fixed. Cells were hybridized with anti-sense probe for histone H3, and incorporated BrdU was visualized with anti-BrdU antibody staining. DNA was stained with DAPI. Digital images for histone H3 mRNA, BrdU, and DNA staining were collected and fluorescent signals for each cell were quantified for each stain. (**A**) Images of histone H3 *in situ* hybridization. High levels of histone message expression were detected in BrdU positive cells as indicated by the arrows. (**B**) BrdU staining levels were plotted against DNA content. Each circle represents an individual cell. The dotted line indicates the cut-off value for BrdU positive cells. (**C**) Values of histone H3 mRNA content divided by DNA content were plotted against DNA content for each cell. The data set is the same as (**B**). Closed triangles represent the cells, which were positive for BrdU in (**B**). Open circles represents BrdU negative cells

transcription. For this purpose, cells were made quiescent by serum starvation for 2 days. Various times after serum addition, nuclei were harvested and the transcription rate of cyclin D1, GAPDH and histone H3 were determined with a nuclear run on assay. GAPDH, as expected, showed a steady transcription rate throughout the cell cycle (Figure 4). Histone H3 transcription, on the other hand, was highest during S phase (Figure 4, 16 h time point) as described before (Delisle *et al*., 1983; Rickles *et al*., 1982). The activity of cyclin D1 transcription was generally constant during the time course we analysed (Figure 4).

Cyclin D1 protein is induced during the S/G2 transition without transcription

To biologically confirm that a change in cyclin D1 transcription is not required for protein induction during the S/G2 transition, we monitored cyclin D1 expression in the presence of a transcription inhibitor. α-Amanitin, which does not inhibit cell cycle progression from S to G2 phase (Adolph *et al*., 1993), is a specific inhibitor of RNA polymerase II. To examine the inhibition efficiency of α-amanitin on mRNA synthesis, incorporation of microinjected BrUTP into mRNA was monitored by immunostaining. Ninety

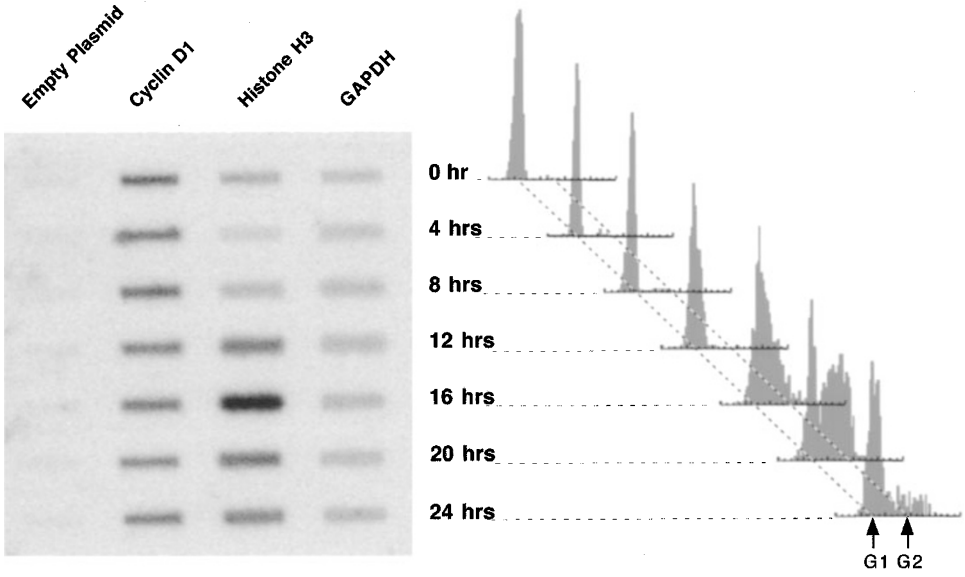

Figure 4 Nuclear run-on assay. NIH3T3 cells were made quiescent by serum starvation for 2 days. At the indicated times after serum addition, nuclei were collected, and nascent RNA was labeled with α-^{32}P-UTP. The labeled RNA from each time point was hybridized to the indicated plasmids containing the cDNA fragment of interest, which were immobilized on a membrane. To monitor the cell cycle at each time point, cells on coverslips were fixed at the time of nuclei harvesting, and stained with DAPI. The histogram of DNA content is shown on the right side of the figure

minutes after BrUTP microinjection in the absence of α-amanitin, BrUTP incorporation was detected in the nucleoplasmic region and nucleoli (Figure 5A, b). Within 20 min of α-amanitin treatment, however, BrUTP incorporation into the nucleoplasmic area was completely blocked (Figure 5A, f), indicating that mRNA synthesis was efficiently suppressed by α-amanitin (Wei *et al*., 1999). The detected BrUTP incorporation into nucleoli was due to ribosomal RNA synthesis mediated by RNA polymerase I (Figure 5A, e and f) (Wei *et al*., 1999). The inhibitory effect of α-amanitin lasted more than 6 h (data not shown).

In order to monitor the effect of this transcription inhibition on cyclin D1 elevation during cell cycle transition from S to G2 phase, we tagged the cells in S phase with a short pulse of BrdU at the beginning of the experiment (Figure 5B). When the pulsed cells were immediately fixed, BrdU-labeled, S phase cells expressed low levels of cyclin D1 protein in comparison to BrdU-negative cells in G1 or G2 phases (Figure 5B, 0 h). When the BrdU pulse was followed by a 6-h-chase period with culture medium without BrdU, the majority of BrdU labeled cells had progressed into G2 phase, and a small fraction of BrdU labeled cells had divided and progressed into G1 phase (Figure 5B, 6h closed triangles). During this cell cycle progression from S to G2 phase, cyclin D1 protein was induced to higher levels. When the culture was chased for 6 h in the presence of α-amanitin, the majority of the BrdU labeled cells progressed into G2 phase and a few progressed into G1 phase (Figure 5B, α-amanitin). The decrease in the number of BrdU positive cells which had progressed into G1 phase, suggests a potential slight delay of cell cycle progression caused by transcription inhibition. Cyclin D1 protein was strongly induced as the cells progressed from S to G2 phase even when mRNA synthesis was inhibited by α-amanitin (Figure 5B, 6 h and α-amanitin). For comparison, anti-Ras antibody was injected into randomly chosen cells (100–150) of an asynchronous culture. Injected cells were identified by staining for injected anti-Ras antibody. To identify the cells in S phase at the time of injection, the cells were pulsed with BrdU prior to injection. After the injection cells were cultured for 6 h with BrdU free medium. Six hours after injection, the majority of BrdU positive cells progressed into G2 phase. In contrast to α-amanitin treatment, neutralization of Ras activity efficiently blocked cyclin D1 protein induction among BrdU positive cells (Figure 5B, anti-Ras), confirming the Ras dependency of cyclin D1 protein induction during cell cycle transition from S to G2 phase (Hitomi and Stacey, 1999b). These data indicate that cyclin D1 protein induction during cell cycle progression from S to G2 phase requires Ras activity but not *de novo* synthesis of message.

The effect of transcription inhibition on cyclin D1 protein production was also examined in cells synchronously reinitiating cell cycle progression from quiescence. This experiment should serve as a control to monitor the potency of α-amanitin, because transcriptional regulation is reported to be involved in cyclin D1 protein induction during reentry into the cell cycle (Albanese *et al*., 1995; Gille and Downward, 1999). Serum starved, quiescent cells were stimulated with serum in the presence or absence of α-amanitin. Cells were fixed and stained for cyclin D1 and DNA at the indicated times after serum addition. Cyclin D1 protein was slightly induced 6 h after serum stimula-

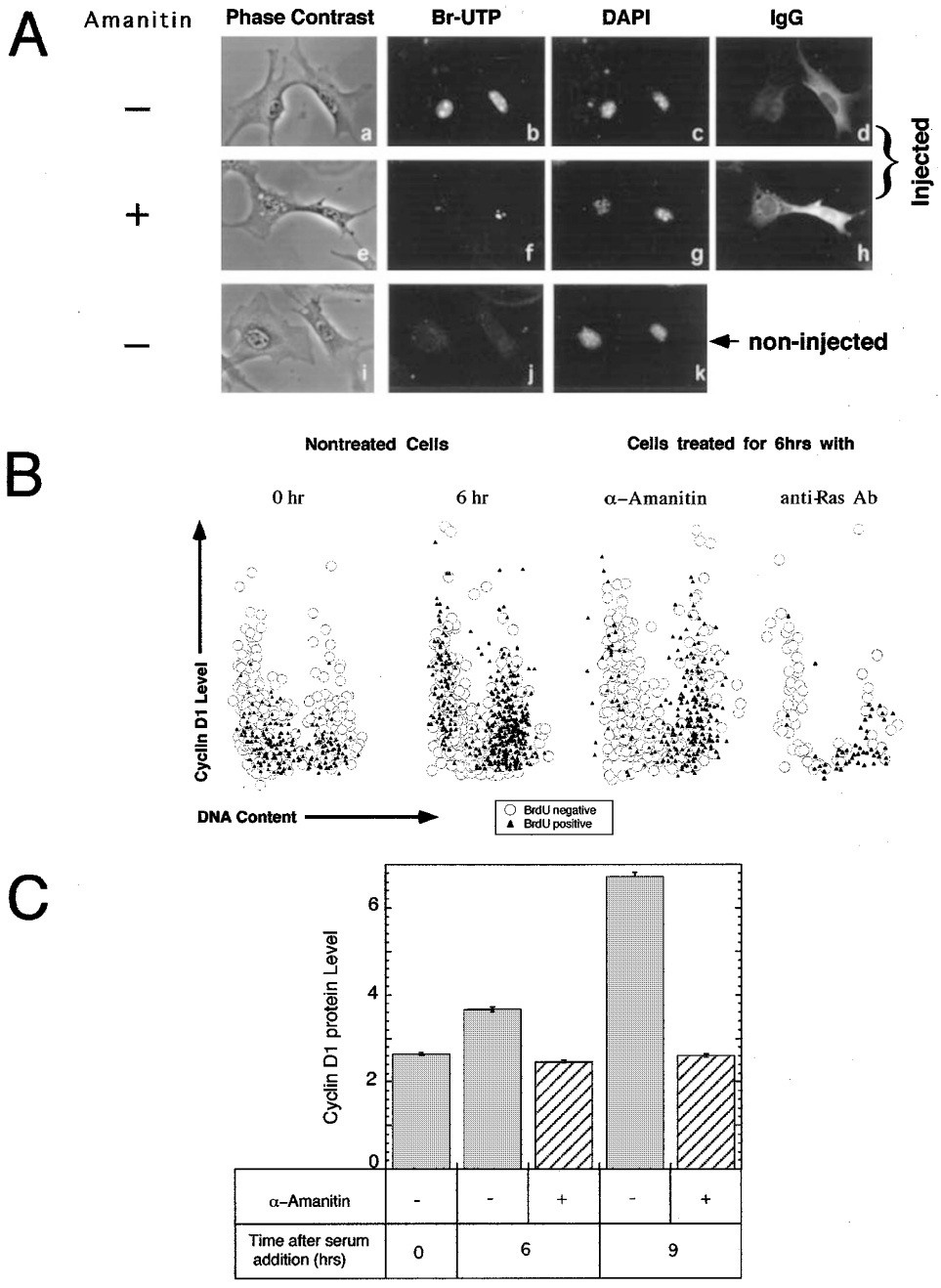

Figure 5 Effect of α-amanitin on mRNA synthesis and Cyclin D1 protein expression. (**A**) NIH3T3 cells were treated with 20 μM α-amanitin (e–h) for 20 min or 6 h (not shown) prior to microinjection of 10 mM BrUTP mixed with marker IgG. Ninety minutes after the injection, cells were fixed and incorporated BrUTP was stained with anti BrdU antibody (b, f, and j). Injected marker IgG (d and h) and DNA (c, g, and k) were also stained. To identify nucleoli, phase contrast pictures were also taken (a, e, and i). As a positive control, non-treated cells were injected with BrUTP and stained (a–d). As a negative control, non-injected cells were also stained (i–k). (**B**) NIH3T3 cells were pulsed with BrdU for 30 min. One plate was fixed immediately (0 h). The other plates were washed thoroughly with fresh medium to remove BrdU and cultured for 6 h with or without α-amanitin treatment or with anti-Ras antibody microinjection. After fixing, cyclin D1 protein and injected IgG were stained with specific antibodies and DNA was stained with DAPI. The fluorescence intensity for each staining was determined by digital image analysis. Cyclin D1 protein level was plotted against DNA content for each cell. Open circles are BrdU negative cells and closed triangles are BrdU positive cells. (**C**) NIH3T3 cells grown on cover slips were made quiescent by serum starvation for 2 days. The cells were stimulated with serum in the presence or absence of 20 μM of α-amanitin. At the indicated times after serum stimulation, cells were fixed and cyclin D1 expression levels were determined by image analysis. Cyclin D1 protein levels of about 500 cells were averaged for each time point. The error bars indicate standard error

tion, and more prominently at 9 h. When the cells were stimulated with serum in the presence of α-amanitin, as expected, cyclin D1 protein induction was completely blocked (Figure 5C), indicating the

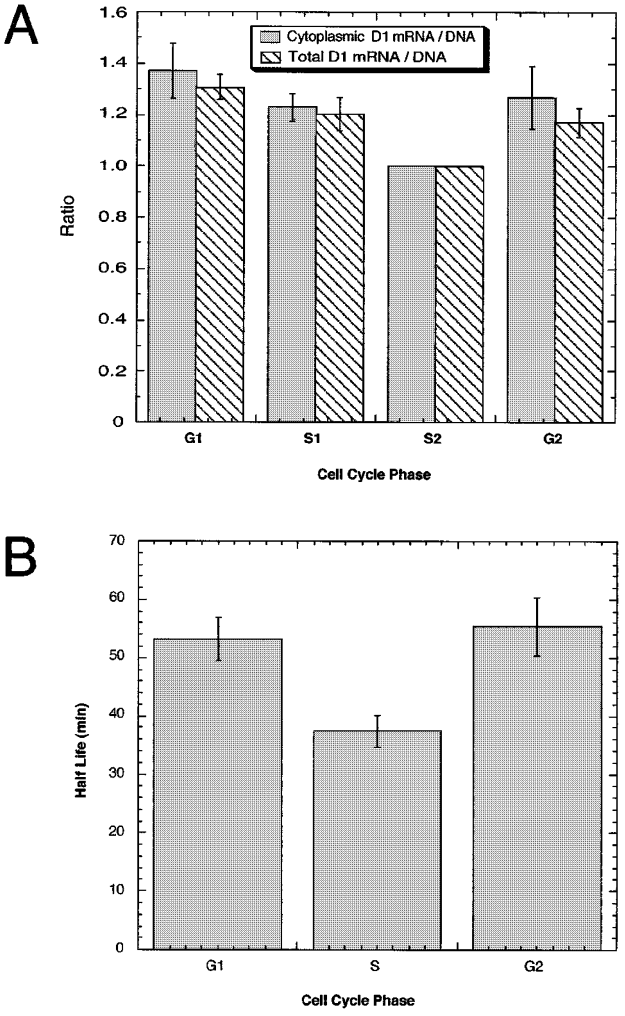

Figure 6 Cytoplasmic expression of cyclin D1 mRNA and protein stability. (**A**) NIH3T3 cells were labeled with BrdU for 15 min, and fixed. Cyclin D1 mRNA was detected with fluorescent *in situ* hybridization. DNA and incorporated BrdU were stained with DAPI and indirect immunofluorescence, respectively. DNA content and BrdU staining intensity of each cell were determined by analysing the digitally captured fluorescent images to determine cell cycle phase. Cyclin D1 mRNA expression in the whole cell (solid bars) or in the extranuclear region (hatched bars) were determined by image analysis and corrected for DNA content. Then the corrected values were normalized to the level of late S phase cells. The data are averages from three independent experiments and standard errors are indicated by error bars. No statistical significance was detected between total and extranuclear cyclin D1 mRNA expression levels. (**B**) NIH3T3 cells were treated with 4 μM cycloheximide for various time up to 1 h. The cells were pulsed with BrdU for 15 min before fixing to identify S phase cells. Cyclin D1 protein and incorporated BrdU were stained with indirect immunofluorescence and DNA was stained with DAPI. Each fluorescence signal was quantified by digital image analysis. The half-life of cyclin D1 protein was determined by analysing the kinetics of cyclin D1 signal decline after cycloheximide addition. The average values of five independent experiments are indicated. The error bars indicate standard errors. The differences of half-life between S and G1 phases, and S and G2 phases are statistically significant (*t*-test, $P<0.01$)

efficiency of inhibition by α-amanitin. This result also indicates that cyclin D1 protein induction during G0/G1 transition requires transcription; in contrast to the induction during the cell cycle transition from S to G2 phase.

Message localization and protein stability

To study the mechanism of post-transcriptional cyclin D1 induction during the S/G2 phase transition, we examined message utilization and/or protein stability. For the efficient expression of cyclin D1 protein, its message has to be exported from the nucleus to the cytoplasm by the action of eukaryotic initiation factor 4E (Rosenwald *et al*., 1995; Rousseau *et al*., 1996). Therefore, we analysed fluorescent *in situ* hybridization images to determine the cell cycle-dependent change in cyclin D1 message localization. Captured digital images were carefully processed so that total cyclin D1 mRNA signal and the signal of cyclin D1 mRNA expressed in the extranuclear region could be determined for individual cells (see Materials and methods). As cells progressed from late S phase to G2 phase, the induction of extranuclear cyclin D1 mRNA expression was slightly greater than that of whole cyclin D1 mRNA. However, the difference was not statistically significant (Figure 6A).

Finally, cyclin D1 protein stability was determined for each cell cycle phase of asynchronous cultures. Cyclin D1 has been reported as an unstable protein. However, to our knowledge, there has been no report of cell cycle dependent change of cyclin D1 protein stability. The half-life of cyclin D1 protein in each cell cycle phase was determined by monitoring the time course of the decline in expression levels after the blockade of *de novo* protein synthesis. Asynchronous cultures of NIH3T3 cells were treated with 2 μM cycloheximide for various times up to 1 h. The concentration of cycloheximide was chosen because it could block more than 90% of *de novo* protein synthesis (Shu *et al*., 1996). The short half life of cyclin D1 protein allowed us to perform experiments with short periods of cycloheximide treatment to minimize the change of this protein expression levels due to cell cycle progression. Cells were labeled with BrdU for 15 min prior to fixing. Incorporated BrdU, cyclin D1, and DNA were stained and the fluorescent intensity of each staining was quantified. As shown in Figure 6B, cyclin D1 half-life is shorter during S phase than during G1 or G2 phase. There was no significant difference of protein stability detected between early S phase and late S phase cells (data not shown). This result indicates that protein stabilization may play a role, at least in part, in the post-translational induction of cyclin D1 during S/G2 cell cycle transition.

Discussion

During continuous cell cycle progression, cyclin D1 protein is expressed at lowest levels during S phase. When cells progress from S to G2 phase, cyclin D1 protein is induced to higher levels in a Ras-dependent

manner, and continues to be expressed at high levels through the next G1 phase (Hitomi and Stacey, 1999b). In this study, we examined the mechanism involved in this cyclin D1 protein induction during the cell cycle transition from S to G2 phase. The cell cycle dependent change in cyclin D1 mRNA levels was very small as compared to the cell cycle associated 2.5–3-fold change in cyclin D1 protein expression. The transcriptional rate of the cyclin D1 gene as determined by run-on assay was almost constant throughout the cell cycle. Cyclin D1 protein was induced during S/G2 transition even when new synthesis of mRNA was inhibition by α-amanitin. All these data indicate that cyclin D1 protein induction in G2 phase is mediated by post-transcriptional mechanisms, and does not require *de novo* mRNA synthesis. This means that cyclin D1 protein induction is mainly mediated either by a translational or a post-translational mechanism. The half-life of cyclin D1 protein was longer in G2 and G1 phase than in S phase. This stability change should play at least some role in transcription-independent cyclin D1 protein induction in G2 phase of continuously cycling cells.

Cyclin D1 is an unstable protein. Its degradation is known to be triggered by phosphorylation of Thr286 by glycogen synthase kinase 3 β (GSK3) (Diehl *et al*., 1998). GSK3 is phosphorylated by AKT and its phosphorylation suppresses GSK3 kinase activity. Since Akt is activated by PI3 kinase activation and PI3 kinase in one of the down stream effector molecules of Ras signaling, it is possible that Ras activity could suppress GSK3 activity through the PI3kinase-Akt pathway resulting in stabilization of cyclin D1 protein. Furthermore, during S phase GSK3 may translocate to the nucleus where cyclin D1 is located. This co-localization would facilitate cyclin D1 degradation during S phase (Diehl *et al*., 1998). It is also reported that this phosphorylation by GSK3 is a signal for cyclin D1 to translocate out of nucleus (Alt *et al*., 2000). Since we measured nuclear expression of cyclin D1 protein by image analysis, such redistribution could be the reason for low expression levels during S phase. However, we could not observe any significant expression of cyclin D1 in the cytoplasmic region at any time during the cell cycle except for the mitotic phase (Hitomi and Stacey, 1999a). Rather, we found that decreased nuclear content of cyclin D1 correlated with total cyclin D1 expression levels determined by Western blot analysis (Hitomi and Stacey, 1999b), indicating that there was an absolute decrease in protein expression during S phase. A similar cyclin D1 protein expression decrease in S phase has been detected by Western blotting during reentry into the cell cycle from quiescence (Baldin *et al*., 1993; Lukas *et al*., 1994a,b). When cyclin D1 is not bound to cdk4, cyclin D1 is also degraded by a GSK3-phosphorylation independent mechanism (Germain *et al*., 2000). Since cyclin D1 associates with its kinase partners to lessor extents during S phase (Sherr *et al*., 1992), such GSK3 independent degradation may keep cyclin D1 protein expression low during S phase.

Translational control is another potential mechanism of post-transcriptional regulation. There are two mechanisms to be considered which may control cyclin D1 translation. One is mTOR and/or PI3 kinase regulated p70S6 kinase dependent control, and the other is PI3 kinase eIF4E mediated control. Importantly, both pathways can potentially be coupled to Ras activity, since Ras can activate PI3 kinase and its targets (Pacold *et al*., 2000; Rodriguez-Viciana *et al*., 1994). The translation efficiency of mRNA possessing a 5′ terminal oligopyrimidine tract (TOP) is subjected to p70S6 kinase activity (Jefferies *et al*., 1997). Since cyclin D1 message contains a putative TOP sequence (Hashemolhosseini *et al*., 1998), its translation could be regulated by the p70S6 kinase pathway (Brown and Schreiber, 1996; Gingras *et al*., 2001). However, p70S6 kinase inhibition did not alter the cyclin D1 synthesis rate in NIH3T3 cells, indicating that this putative TOP sequence is not biologically functional (Hashemolhosseini *et al*., 1998). Another potential mechanism is through eIF4E (eukaryotic initiation factor 4 E) (Brown and Schreiber, 1996; Gingras *et al*., 2001), which could be activated by Ras (Rinker-Schaeffer *et al*., 1992). The translation efficiency of cyclin D1 is known to be controlled by the activity of eIF4E (Rosenwald *et al*., 1993). eIf4E facilitates cyclin D1 mRNA export from the nucleus to the cytoplasm resulting in increased production of cyclin D1 (Rosenwald *et al*., 1995; Rousseau *et al*., 1996). When determined the cyclin D1 message subcellular distribution by fluorescent *in situ* hybridization, there was no significant cell cycle-dependent increase in the cytoplasmic expression of cyclin D1 message compared to total cyclin D1 message. However, the results obtained by Hashemolhosseini *et al*. (1998) together with our current data do not rule out the involvement of other translational control mechanisms in cell cycle dependent fluctuation of cyclin D1 protein expression.

This Ras-dependent, post-transcriptional cyclin D1 protein induction in G2 phase is fundamentally different from cyclin D1 protein induction during reentry into the cell cycle. Cyclin D1 protein as well as mRNA are expressed at low levels is quiescent cells. As they reinitiate the cell cycle upon mitogenic stimulation, both message and protein levels gradually increase (Sherr, 1995). This process requires Ras activity and its downstream signaling pathways (Albanese *et al*., 1995; Gille and Downward, 1999); and these pathways are believed to activate cyclin D1 transcription (Amanatullah *et al*., 2001). As expected, cyclin D1 protein induction during cell cycle reentry was completely inhibited by the transcription inhibitor, α-amanitin. On the other hand, during the transition from S to G2 phase of continuous cell cycle progression, cyclin D1 was induced in the presence of this transcription inhibitor. During continuous cell cycle progression, changes in cyclin D1 protein stability play an important role in regulation of cyclin D1 expression, as indicated by the half life differences among cell cycle phase. These results indicate that, in

addition to a temporal difference in Ras requirement (Hitomi and Stacey, 1999a), there is a mechanistic difference in the way Ras induces cyclin D1 protein between continuously cycling cells and in cells reentering the cell cycle.

Many post-transcriptional mechanisms regulating cyclin D1 protein expression have been reported. For examples, growth suppressive treatments decreased cyclin D1 protein synthesis with minimal changes in message levels (Brewer and Diehl, 2000; Mettouchi *et al*., 2001; Muise-Helmericks *et al*., 1998; Palakurthi *et al*., 2000; Pervin *et al*., 2001). Fumonisin B1, a carcinogenic mycotoxin, stabilizes cyclin D1 protein resulting in high levels of protein expression without a change in message levels (Ramljak *et al*., 2000). Growth suppressive chemicals can also destabilize cyclin D1 message and/or protein (Agami and Bernards, 2000; Dufourny *et al*., 2000, Hashemolhosseini *et al*., 1998; Lin *et al*., 2000). It will be interesting to determine if these events are controlled by the same post-transcriptional mechanism as the cyclin D1 induction during G2 phase.

This study reveals that in continuously cycling cells, the Ras-dependent cyclin D1 induction during the transition from S to G2 phase does not require *de novo* mRNA synthesis; and moreover, a change of protein stability may be involved in this induction. We have recently found that oncogenic Ras only took 3 h to induce cyclin D1 protein in G2 phase cells of an asynchronous culture. On the other hand, it took 6–9 h to induce cyclin D1 protein when cells were quiescent (Sa *et al*., 2002). Therefore, it is possible that this post-transcriptional induction of cyclin D1 protein allows for the rapid control necessary for rapid cell cycle progression.

Materials and methods

Materials

Plasmids containing the mouse histone H3 coding sequence (ATCC #63143) and glyceraldehyde phosphate dehydrogenase (GAPDH) cDNA (ATCC #285241) were obtained from the American Type Culture Collection (Manassas, VA, USA). Trizol and pZErO-2 plasmid were purchased from Invitrogen (Carlsbad, CA, USA). α-^{32}P-UTP was purchased from ICN (Irvine, CA, USA). A BrdU (5-Bromo-2′-deoxyuridine) staining Kit was obtained from Zymed (South San Francisco, CA, USA). Mouse monoclonal anti-BrdU antibody, SP6/T7 DIG RNA labeling Kit, DIG detection Kit, and T3 DNA dependent RNA polymerase were products of Roche (Indianapolis, IA, USA). Anti-cyclin D1 Ab (72-13G) was obtained from Santa Cruz Biotechnology (Santa Cruz, CA, USA). Non-immune mouse and Rat IgG, biotinylated-anti-digoxin antibody, anti-digoxin antibody-alkaline phosphatase conjugate, 5-bromouridine 5′-triphosphate (BrUTP) and α-amanitin were products of Sigma (St. Louis, MO, USA). Fluorochrome labeled secondary antibodies, and Cy2-streptoavidine were purchased from Jackson Immunoresearch (West Grove, PA, USA). 4′,6-diamidino-2-phenylindole, dilactate (DAPI) was obtained from Molecular Probes (Eugene, OR, USA).

In situ *hybridization*

Genomic clones containing the cyclin D1 3′ untranslated region (UTR) (Smith *et al*., 1995) (generous gift from Dr Clive Dickson), or the histone H3 coding region (ATTC #63143) were excised by restriction enzymes (*Eco*RI/*Xba*I) and subcloned into the corresponding pZErO-2 vector multiple cloning sites flanked by SP6 and T7 promoters. Mouse GAPDH cDNA flanked by T3 and T7 promoters (ATCC #285241) was obtained from ATCC. After the plasmids were linearized with an appropriate restriction enzyme digestion, digoxigenin labeled riboprobes in both sense and anti-sense orientations were synthesized with an *in vivo* DIG RNA Labeling Kit using T3, T7 or SP6 polymerase according to the manufacturer's instructions. To visualize the mRNA of interest, fluorescent *in situ* hybridization was performed accordingly with modification (Dirks, 1996; Raap *et al*., 1997). The cells grown on coverslips were fixed with 3.7% formaldehyde in 0.9% (w/v) NaCl containing 5% (v/v) acetic acid. After treatment with 0.1 N HCl and anhydrous acetic acid accordingly (Raap *et al*., 1997), monolayers were prehybridized with hybridization solution Dig detection kit at 37°C for overnight. The probes were used as they were transcribed *in vitro* without alkaline hydrolysis. After hybridization at 60°C for 1–2 days, without post-hybridization nuclease treatment, the hybridized probe was visualized using biotinylated anti-digoxin antibody (1 : 100 dilution) coupled to the Cy-3-TSA signal amplification kit (NEN, Boston, MA, USA).

Microinjection and immunofluorescent staining

To assess the effect of α-amanitin, an inhibitor of DNA dependent RNA polymerase II, 10 mM BrUTP was co-microinjected with marker IgG after 20 min or 6 h of pretreatment with α-amanitin (20 μM). Ninety minutes after the injection, cells were fixed with 3.7% paraformaldehyde containing 5% acetic acid and 0.9% NaCl. After three rinses with PBS, cells were permeabilized with 70% ethanol and incorporated Br-uridine into RNA was detected by indirect immunofluorescence using anti-BrdU antibody (Roche) according to the manufacturer's instructions. To minimize the degradation of BrUTP labeled RNA, RNase free solutions were used for staining and antibodies were diluted with 1% (w/v) hybridization blocking solution (Roche). Anti-Ras antibody injection was performed as described (Hitomi and Stacey, 1999a,b, 2001).

Cyclin D1 protein was stained with a specific monoclonal antibody G72-13 (4 μg/ml) followed by Cy3 labeled anti-mouse secondary antibody (Hitomi and Stacey, 1999b). To determine the background fluorescent levels of immunostaining, non-immune mouse IgG was used as primary antibody at a matching concentration (4 μg/ml). To detect incorporated BrdU, the cells stained for cyclin D1 were re-fixed with cold methanol. Then, incorporated BrdU was stained accordingly to the instruction for BrdU staining Kit (Zymed), with two modifications: (1) 1 mg/ml of non-immune mouse IgG was included in the blocking solution to minimize the nonspecific staining; (2) Cy2 labeled streptavidin was used for visualization. To detect incorporated BrdU in fluorescent *in situ* hybridization analysis, polyclonal sheep anti-BrdU Ab (Fitzgerald Industries International, Concord, MA, USA) was used instead of the antibody provided in the Kit.

To determine the half life of cyclin D1 protein for each cell cycle phase, asynchronous NIH3T3 cultures were treated with 2 μM cycloheximide for various times up to 1 h. Just prior to fixing, the cells were labeled with BrdU for 15 min to

identify S phase cells. DNA, cyclin D1, and incorporated BrdU were stained with DAPI and immunofluorescence as described above. Average values of cyclin D1 staining levels were determined for each cell cycle phase using digital image analysis after subtracting the background staining levels. The decline of cyclin D1 expression was monitored as function of time after cycloheximide treatment.

Image analysis

Fluorescent microscopic digital images were captured and analysed to quantify fluorescent signals of individual cells (Hitomi and Stacey, 1999b). In order to determine the fluorescent intensity of the signals located in cytoplasm, we devised a way to define the whole cell area for measurement, rather than the nuclear region measurement we have described (Hitomi and Stacey, 1999b). To determine the mRNA expression levels in synchronous culture, integrated fluorescent signals of photographed fields were divided by the number of the cells in the fields determined by image analysis of DAPI staining. For fluorescent *in situ* hybridization measurements of cells from asynchronous cultures, minimal thresholding of the DAPI images defined the whole cell area. This was possible because during the fluorescent *in situ* hybridization procedure, the cytoplasmic RNA was preserved and faintly stained with DAPI.

Nuclear run-on assay

To determine transcription rate, nuclear run-on assays were performed as described (Srivastava and Schonfeld, 1994) with slight modification. NIH3T3 cells were synchronized by serum starvation for 2 days. At the indicated times after serum stimulation, cells were trypsinized. About 1×10^8 cells per assay were incubated with hypotonic buffer (20 mM Tris-HCl, pH 8.0, containing 4 mM $MgCl_2$, 6 mM, $CaCl_2$, and 0.5 mM DTT) for 5 min on ice. Cells were resuspended in 0.6 M sucrose solution containing 0.2% Nonidet p-40 and 0.5 mM DTT, and nuclei were released with 10 strokes of a tight fitting pestle through glass tissue grinder. The nuclei were collected by centrifugation at 1500 *g* for 10 min at 4°C and resuspended in 50 mM Tris HCl buffer, pH 8.3, containing 5 mM $MgCl_2$, 0.1 mM EDTA, and 40% glycerol, and frozen at −80°C. The thawed nuclei were incubated with a same volume of reaction buffer (20 mM Tris HCl, pH 8.0, 10 mM $MgCl_2$, 0.6 M KCl, 2 mM DTT, 0.4 mM EDTA and 4 mM of each ATP, GTP, CTP and UTP (50 μCi/sample of labeled α-^{32}P-UTP) at 30°C for 20 min. Labeled RNA was extracted with Trizol and radioactivity was determined by liquid scintillation counting. Each extract was normalized to radioactivity and hybridized to target sequences immobilized on a nylon membrane at 48°C overnight. The membrane was washed with $0.2 \times$ SSC at 45°C. The intensity of hybridized radiolabeled mRNA was determined by Phosphor Imager analysis. The alkaline denatured target DNA sequences, cyclin D1 3′ UTR subcloned into pZErO-2 vector, histone H3 coding region, and GAPDH cDNA containing plasmids were immobilized on nylon membrane by slot blotting followed by UV cross-linking. To monitor nonspecific hybridization, empty pZErO-2 vector was also blotted on the membrane.

Northern blotting

Steady state levels of mRNA expression were determined by Northern Blotting (Shu *et al*., 1996). Digoxigenin labeled riboprobes were used to detect blotted mRNA. Hybridized probe was detected with anti-digoxin Ab conjugated with alkaline phosphatase (Sigma) coupled to a chemiluminescent substrate (Amersham Pharmacia, Piscataway, NJ, USA). The signal intensity was determined with a Storm Imager (Molecular Dynamics, Sunnyvale, CA, USA).

Acknowledgements
We thank Clive Dickson for providing us a mouse cyclin D1 genomic clone. We are also grateful for Akiko Nishiyama for technical advice, Jyoti Harwalker, Jeff Nye and Brandon Abood for helping in image analysis, and William C Stacey for reviewing the manuscript. This work was supported by NIH Grants GM52271 and CA92194.

References

Adolph S, Brusselback S and Muller R. (1993). *J. Cell Biol. Sci.,* **105,** 113–122.
Agami R and Bernards R. (2000). *Cell,* **102,** 55–66.
Albanese C, Johnson J, Watanabe G, Eklund N, Vu D, Arnold A and Pestell RG. (1995). *J. Biol. Chem.,* **270,** 23589–23597.
Alt JR, Cleveland JL, Hannink M and Diehl JA. (2000). *Genes Dev.,* **14,** 3102–3114.
Amanatullah DF, Zafonte BT, Albanese C, Fu M, Messiers C, Hassell J and Pestell RG. (2001). *Methods Enzymol.,* **333,** 116–127.
Baldin V, Lukas J, Marcote MJ, Pagano M and Draetta G. (1993). *Genes Dev.,* **7,** 812–821.
Brewer JW and Diehl JA. (2000). *Proc. Natl. Acad. Sci. USA,* **97,** 12625–12630.
Brown EJ and Schreiber SL. (1996). *Cell,* **86,** 517–520.
DeGregori J, Kowalik T and Nevins JR. (1995). *Mol. Cell. Biol.,* **15,** 4215–4224.
DeLisle AJ, Graves RA, Marzluff WF and Johnson LF. (1983). *Mol. Cell. Biol.,* **3,** 1920–1929.
Diehl JA, Cheng M, Roussel FM and Sherr CJ. (1998). *Genes Dev.,* **12,** 3499–3511.
Dirks RW. (1996). *Histochem. Cell Biol.,* **106,** 151–166.
Dirks RW and Raap AK. (1995). *Histochem. Cell Biol.,* **104,** 391–395.
Dufourny B, van Teeffelen HA, Hamelers IH, Sussenbach JS and Steenbergh PH. (2000). *J. Endocrinol.,* **166,** 329–338.
Evan GI and Vousden KH. (2001). *Nature,* **411,** 342–348.
Germain D, Russell A, Thompson A and Hendley J. (2000). *J. Biol. Chem.,* **275,** 12074–12079.
Gille H and Downward J. (1999). *J. Biol. Chem.,* **274,** 22033–22040.
Gingras AC, Raught B and Sonenberg N. (2001). *Genes Dev.,* **15,** 807–826.
Hann SR, Thompson CB and Eisenman RN. (1985). *Nature,* **314,** 366–369.
Hashemolhosseini S, Nagamine Y, Morley SJ, Desrivieres S, Mercep L and Ferrari S. (1998). *J. Biol. Chem.,* **273,** 14424–14429.
Hitomi M and Stacey DW. (1999a). *Mol. Cell. Biol.,* **19,** 4623–4632.
Hitomi M and Stacey DW. (1999b). *Curr. Biol.,* **9,** 1075–1084.

Hitomi M and Stacey DW. (2001). *FEBS Lett.,* **490,** 123–131.
Jefferies HB, Fumagalli S, Dennis PB, Reinhard C, Pearson RB and Thomas G. (1997). *EMBO J.,* **16,** 3693–3704.
Kotelnikov V, Cass L, Coon JS, Spaulding D and Preisler HD. (1997). *Clin. Cancer Res.,* **3,** 669–673.
Kovary K and Bravo R. (1992). *Mol. Cell. Biol.,* **12,** 5015–5023.
Lin S, Wang W, Wilson GM, Yang X, Brewer G, Holbrook NJ and Gorospe M. (2000). *Mol. Cell. Biol.,* **20,** 7903–7913.
Lukas J, Jadayel D, Bartkova J, Nacheva E, Dyer MJS, Strauss M and Bartek J. (1994a). *Oncogene,* **9,** 2159–2167.
Lukas J, Pagano M, Staskova Z, Draetta G and Bartek J. (1994b). *Oncogene,* **9,** 707–718.
Mettouchi A, Klein S, Guo W, Lopez-Lago M, Lemichez E, Westwick JK and Giancotti FG. (2001). *Mol. Cell,* **8,** 115–127.
Muise-Helmericks RC, Grimes HL, Bellacosa A, Malstrom SE, Tsichlis PN and Rosen N. (1998). *J. Biol. Chem.,* **273,** 29864–29872.
Mulcahy LS, Smith MR and Stacey DW. (1985). *Nature,* **313,** 241–243.
Pacold ME, Suire S, Perisic O, Lara-Gonzalez S, Davis CT, Walker EH, Hawkins PT, Stephens L, Eccleston JF and Williams RL. (2000). *Cell,* **103,** 931–943.
Palakurthi SS, Fluckiger R, Aktas H, Changolkar AK, Shahsafaei A, Harneit S, Kilic E and Halperin JA. (2000). *Cancer Res.,* **60,** 2919–2925.
Pardee AB. (1989). *Science,* **246,** 603–608.
Pervin S, Singh R and Chaudhuri G. (2001). *Proc. Natl. Acad. Sci. USA,* **98,** 3583–3588.
Raap AK, van de Rijke FM and Dirks RW. (1997). *Methods Mol. Biol.,* **75,** 367–375.
Ramljak D, Calvert RJ, Wiesenfeld PW, Diwan BA, Catipovic B, Marasas WFO, Victor TC, Anderson LM and Gelderblom WCA. (2000). *Carcinogenesis,* **21,** 1537–1546.
Rickles R, Marashi F, Sierra F, Clark S, Wells J, Stein J and Stein G. (1982). *Proc. Natl. Acad. Sci. USA,* **79,** 749–753.
Rinker-Schaeffer C, Austin V, Zimmer S and Rhoads RE. (1992). *J. Biol. Chem.,* **267,** 10659–10664.
Rodriguez-Viciana P, Warne PH, Dhand R, Vanhaesebroeck B, Gout I, Fry MJ, Waterfield MD and Downward J. (1994). *Nature,* **370,** 527–534.
Rosenwald IB, Kaspar R, Rousseau D, Gehrke L, Leboulch P, Chen JJ, Schmidt EV, Sonenberg N and London IM. (1995). *J. Biol. Chem.,* **270,** 21176–21180.
Rosenwald IB, Lazaris KA, Sonenberg N and Schmidt EV. (1993). *Mol. Cell. Biol.,* **13,** 7358–7363.
Rousseau D, Kaspar R, Rosenwald I, Gehrke L and Sonenberg N. (1996). *Proc. Natl. Acad. Sci. USA,* **93,** 1065–1070.
Sa G, Hitomi M, Harwalker J, Stacey A, Chen G and Stacey DW. (2002). *Cell Cycle,* **1,** 50–58.
Sherr CJ. (1995). *Trends Biochem. Sci.,* **20,** 187–190.
Sherr CJ, Matsushime H and Roussel MF. (1992). *Ciba Found. Symp.,* **170,** 209–219.
Shu J, Hitomi M and Stacey DW. (1996). *Oncogene,* **13,** 2421–2430.
Sicinski P, Donaher JL, Parker SB, Li T, Fazeli A, Gardner H, Haslam SZ, Bronson RT, Elledge SJ and Weinberg RA. (1995). *Cell,* **82,** 621–630.
Smith R, Peters G and Dickson C. (1995). *Genomics,* **25,** 85–92.
Srivastava RAK and Schonfeld G. (1994). *Methods Mol. Biol.,* **31,** 281–288.
Stacey DE, Chen G and Hitomi M. (2000). *Mol. Cell. Biol.,* **20,** 9127–9137.
Stacey DW, Hitomi M, Kanovsky M, Gan L and Johnson EM. (1999). *Oncogene,* **18,** 4254–4261.
Thompson CB, Challoner PB, Neiman PE and Groundine M. (1985). *Nature,* **314,** 363–366.
Vogelstein B, Lane D and Levine AJ. (2000). *Nature,* **408,** 307–310.
Wei X, Somanathan S, Samarabandu J and Berezney R. (1999). *J. Cell Biol.,* **146,** 543–558.
Yan Z, DeGregori J, Shohet R, Leone G, Stiliman B, Nevins JR and Williams RS. (1998). *Proc. Natl. Acad. Sci. USA,* **95,** 3603–3608.